

Conversion of standard induction machines to permanent magnet synchronous machines with higher efficiency

Journal:	<i>IET Electric Power Applications</i>
Manuscript ID:	Draft
Manuscript Type:	Research Paper
Date Submitted by the Author:	n/a
Complete List of Authors:	Sergeant, Peter; Ghent University, Department of Electrical Energy, Systems and Automation; University College Ghent, Department of Electrotechnology Hofman, Isabelle; University College Ghent, Department of Electrotechnology Van den Bossche, Alex; Ghent University, EELAB, EESA, IR08
Keyword:	PERMANENT MAGNET MACHINES, INDUCTION MOTORS, ASYNCHRONOUS MACHINES, LOSSES

SCHOLARONE™
Manuscripts

Conversion of standard induction machines to permanent magnet synchronous machines with higher efficiency

Peter Sergeant^{1,2}, Isabelle Hofman¹, and Alex Van den Bossche²

¹Dept. Electrotechnology, Faculty of Applied Engineering Sciences, University College Ghent,
Schoonmeersstraat 52, B-9000 Ghent, Belgium

²Dept. of Electrical Energy, Systems and Automation, Ghent University,
Sint-Pietersnieuwstraat 41, B-9000 Ghent, Belgium

E-mail: Peter.Sergeant@UGent.be

Abstract

To increase the efficiency of cheap and robust commercial induction machines, especially at part load and speed, these machines are converted into synchronous machines in a fast, cheap and easy way. The stators are not changed at all; only the rotors are modified. The appropriate size of the rotor iron and the magnets is found by using finite element software. The robustness and reliability are unchanged because the stators, the shafts and the bearings are not modified. The resulting synchronous machines still have a rather low torque to weight ratio, but they have low rotor losses, a good power factor and high efficiency.

Two induction machines with approximately the same outer dimensions (a 2-pole 3 kW machine and a 6-pole 1.5 kW machine) were converted into synchronous machines by different production techniques for the rotor. The efficiency maps were simulated and measured for sinusoidal waveforms and for pulse width modulation supply. For both machines, the peak efficiency increases by 2% and 11% respectively, and the average efficiency (between 0.5 and 1 times nominal torque, and 0.5 and 1 times nominal speed) by 2% and 15%. Conversion of induction machines with many poles to synchronous machines improves the efficiency much more than conversion of two-pole induction machines.

Keywords: Permanent magnet machines, Induction motors, Asynchronous machines, Losses

1 Introduction

Standard induction machines (IM) are produced in huge quantities, causing their price to be very low. The efficiency of very large induction machines is high, but the efficiency of smaller machines is much lower. Especially at low speed and power, the efficiency is significantly lower than in the optimal operating point. Efforts are done to increase the efficiency of induction machines on the market: in 2008, the IEC 60034-30 standard was approved [1]. In this standard, efficiency classes IE1, IE2 and IE3 are defined for direct-on-line induction motors up to 375 kW. This standard defines minimum efficiency values for the machine directly connected to the grid. The difference between the several classes is obtained by amongst others better magnetic material and optimized geometry of stator and rotor. To understand the difference between the classes, [2] shows iso efficiency contours for three induction machines of 11 kW and 1500 rpm, having class IE1, IE2 and IE3 respectively. The iso efficiency contours show the efficiency

in a wide speed and torque range, not only in direct on line operation. This is useful because more and more machines are operated by a variable speed drive. It is found that IE3 has a 2% efficiency increase compared to IE1 in a wide speed and torque operating range. However, the magnetizing current – which causes extra copper losses in the stator – and the Joule losses in the rotor bars cannot be avoided.

Permanent magnet synchronous machines (PMSM) have almost no Joule losses in the rotor: the currents induced in the magnets and the back iron can be small if the machine is well designed (small slot openings, several slots per pole per phase to obtain a nearly sinusoidal mmf (magneto motive force) distribution along the air gap, segmented magnets, ...). Furthermore, a synchronous machine does not need magnetizing current in the stator, so that for the same voltage, the same active power can be produced with a lower stator current. It is expected that converting an IE1 induction machine to a synchronous machine can increase the efficiency even more than replacing it by an IE3 machine.

In literature, the energy efficiency of permanent magnet synchronous motors and induction motors has been compared. In [2], an IE3 induction motor of 4 kW is compared with a PMSM in the same power range. The efficiency improvement turned out to be at least 4.5%, even much more for low speed and low torque. In [3], a self-starting PMSM for compressor drives is designed. The authors found for the PMSM – compared with an isometric induction motor – efficiency improvements of 9% and 7% for rated operation under 50 Hz and 60 Hz, respectively. The power factors also increased by 17% and 10% for the same rated operations. This reduces also the losses in the converter. In [4], two water-cooled machines with the same nominal power (85 kW) and dimensions are compared regarding their energy efficiency: an induction motor with efficiency $\eta = 92.6\%$ and an interior permanent magnet synchronous motor with efficiency $\eta = 95.8\%$. From the presented calculation results, the efficiency of the synchronous machine turns out to be significantly higher.

Another example shows that a PMSM is not always better than an IM. In [5], the performances of 4-pole and 2-pole solid-rotor induction machines for high speed (29100 rpm) are compared with the measured performance of a PMSM of the same active volume. The simulation results show that a 2-pole solid rotor induction motor has a larger torque density and is a better candidate for high speed drives. At very high speed, the induction motor can have a better performance than a PMSM.

In the speed range that most induction and synchronous machines operate (0-1500 rpm or 0-3000 rpm), many examples from literature show that a PMSM may be more efficient than an induction machine. However, the price of such a machine is much higher. Therefore, in this paper, we check if a conventional IM can be converted to a PMSM, for almost no extra material cost except the price of the magnets and with a minimum of effort. As rare earth magnets are expensive, the amount of magnets is chosen as low as acceptable. The possibility to use cheaper ferrite magnets was investigated, but turned out to result in a too low flux level in the machines. The stator is unchanged, and the rotor is replaced by a modified

one. For the rotor, different magnet assemblies can be implemented like in [6], but for the considered machines, we choose a rectangular array of small block-shaped magnets. We study what the magnet pole-arc to pole-pitch ratio and the air gap should be in order to have a properly designed machine, even if the stator cannot be optimized.

Two induction machines are converted to synchronous machines, both numerically and experimentally: a 3 kW, 2-pole machine and a 1.5 kW, 6-pole machine. The original and converted machines are compared regarding their efficiency. For each machine, a different production technique for the rotor was used. Also a different control technique was used: the 3.0 kW machine was used in open loop on a perfectly sinusoidal three phase grid; the 1.5 kW machine was controlled in closed loop (with a position encoder) by a frequency converter with pulse width modulation (PWM).

2 Converting an induction machine to a synchronous machine

2.1 New rotor back iron on the same shaft

A first possibility to make the PM rotor is to completely remove the rotor iron and the aluminium cage by cutting with a lathe. Then, a new cylinder is made with a suitable diameter. The internal radius of the cylinder is such that it fits on the original shaft of the machine. By using the original shaft, the risk of misalignment or eccentricity of a new shaft is avoided. The cylinder can be fixed on the shaft by gluing or via a wedge. Conventional and cheap block shaped NdFeB magnets are glued on the outside of the cylinder: see Fig. 1.



Figure 1: The rotor of the two pole machine during construction, with one magnet pole (7×4 rectangular magnets with dimensions $20 \times 10 \times 5$ mm) glued.

The dimensions of the magnets should be carefully determined as explained in section 3. It is preferred to use small pieces of magnets for three reasons. First, the small wedges between the flat magnet surface and the curved cylinder are useful for gluing. The thickness of the glue layer is somewhat thicker near the edge of the magnets, which guarantees sufficient mechanical elasticity in case of temperature changes. Secondly, the eddy currents in the magnets are smaller as the magnet is naturally segmented. Thirdly, conventional rectangular magnets are easy to order and cheaper (in low quantities) than complex shaped magnets. After the magnets are fixed to the rotor, optionally a fibre glass tape can be added around the

rotor. This protects the magnets from centrifugal forces, but increases the air gap thickness.

The above approach was chosen for *the 3 kW 2-pole machine*. As this machine has two poles, it could be made by two large curved magnets. However, it was preferred to realize each of the two magnet poles by 28 small block shaped magnets: 7 next to each other along the circumference, and 4 in axial direction: see Fig. 2 and the photo in Fig. 1 where one magnet pole is glued.

2.2 Use the original rotor lamination as back iron

The PM rotor can also be made in a different way. The rotor iron is only partially removed by cutting with a lathe: the thickness of the removed zone equals the magnet thickness, possibly slightly increased to have a larger air gap. Usually, the magnet thickness is smaller than the slot depth in the rotor of the IM. This means that the short-circuited rotor bars are not completely removed. They can be either further removed in a mechanical way, or be kept. As the PMSM rotates at synchronous speed, the short-circuited rotor bars will not cause much losses in the rotor. However, the bars are non-magnetic, causing an additional reluctance and possibly local saturation of rotor teeth. The total magnetic flux in the machine may be reduced if the cage is not entirely removed.

The above approach was chosen for *the 1.5 kW 6-pole machine*. The 6 magnet poles consist of 16 small rectangular magnets each: 4 next to each other along the circumference, and 4 in axial direction. The cage was not completely removed.

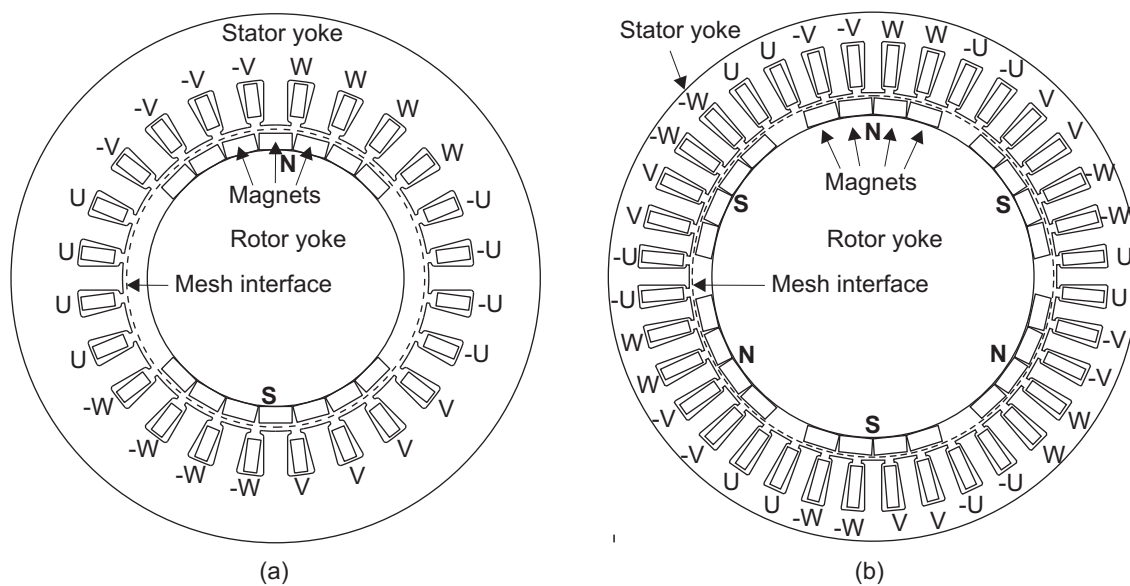


Figure 2: Geometry of (a) the 3 kW, 2-pole machine and (b) the 1.5 kW, 6-pole machine. Geometrical dimensions and electromagnetic properties are in Table 1.

3 Numerical model to predict the efficiency of the converted machine

3.1 Finite element model

The numerical model is a transient 2D Finite Element model (FEM) that uses the moving mesh technique. The unknown is the magnetic vector potential. The torque is computed by the Maxwell stress tensor. For the stator and rotor iron, the magnetic characteristic was experimentally determined as explained in the next section. The geometry of both machines used in FEM is shown in Fig. 2, and the dimensions are given in Table 1. The line in the air gap is the interface between the fixed mesh of the stator and the rotating mesh of the rotor.

Table 1: Data and properties of the two induction and synchronous machines

	Property	3.0 kW, 2-pole	1.5 kW, 6-pole
Performance	Nominal speed IM	2870 rpm	910 rpm
	Nom. phase current (400 V, Y)	5.96 A	3.90 A
	Nom. power factor IM	0.87	0.73
Stator	Outer diameter	160 mm	158.4 mm
	Inner diameter	92.6 mm	109.9 mm
	Copper resistance	2.10 Ω	5.11 Ω
	Sheet thickness	0.5 mm	0.5 mm
	Stack width	95.3 mm	80.7 mm
	Number of slots	24	36
	Turns per slot	43	60
Rotor IM	Number of poles	2	6
	Outer diameter	91.4 mm	109.4 mm
	Shaft diameter	35 mm	30 mm
	Number of slots	28	33
	Radial height of slots	20 mm	15.3 mm
	Air gap IM	0.6 mm	0.25 mm
	Rotor PMSM	Iron yoke diameter	77.6 mm
Number of magnets per pole		7 \times 4	4 \times 4
Magnet pole angle		103 $^\circ$	142 $^\circ$
Magnet (radial) thickness		5 mm	5 mm
Magnet width		10 mm	10 mm
Magnet permeability		μ_0	μ_0
Magnet remanent B		1.05 T	1.05 T
Air gap PMSM	2.5 mm	1.7 mm	

For the 3 kW 2-pole machine, we choose conventional rectangular magnets of 10 mm width, 20 mm length and 5 mm thickness. The grade is 35 SH, with a remanence of 1.17 to 1.21 T (ambient temperature) and a maximal temperature of 150 $^\circ$ C. At steady state temperature, a remanence of 1.05 T was used. To obtain the highest possible torque, it is common practice to glue magnets along for example 80% of the pole pitch, and to minimize the air gap. However, it was observed from FEM that the stator

yoke – which is not designed for a PMSM – completely saturates, even in absence of stator current. Furthermore, we prefer to use a rather low amount of magnets for economic reasons. Therefore, only 60 % of the pole pitch is covered with magnets (less than 110 electrical degrees). Even then, a quite large air gap can be chosen, so that several layers of epoxy impregnated fibre glass tape can be added to withstand the centrifugal forces at 3000 rpm. The typical induction in the yoke is now about 1.4 T, in no-load conditions.

For the 1.5 kW 6-pole machine, we choose the same conventional rectangular NdFeB magnets. In contrast with the other machine, we choose a higher magnet to pole pitch ratio of 142 electrical degrees resulting in a rather high no-load induction level in the yoke (1.7 T). As the stator cannot be optimized, an optimal design to achieve a maximum torque density like in [7] is not possible. Nevertheless, the torque density increases compared to the induction machine – more torque per ampere stator current – and also the efficiency increases significantly as shown in section 4.

3.2 Calculation of the losses

The losses in the stator iron are dependent on the induction $B(t)$ and its time derivative dB/dt in each point of the stator iron. The waveforms $B(t)$ in the stator iron are computed in the transient 2D FEM computation for no-load and for several load conditions. A posteriori, a loss model is applied to compute the iron losses in the stator. The following paragraphs explain the loss model.

Firstly, loss measurements of the stator iron were done. As cutting processes and mechanical stresses have a strong influence on the behaviour of the magnetic material [8], hysteresis loops were measured on the material *inside* the machine. Therefore, the rotor was removed from the machine, and a measurement winding and excitation winding were added around the stator yoke: see Fig. 3.

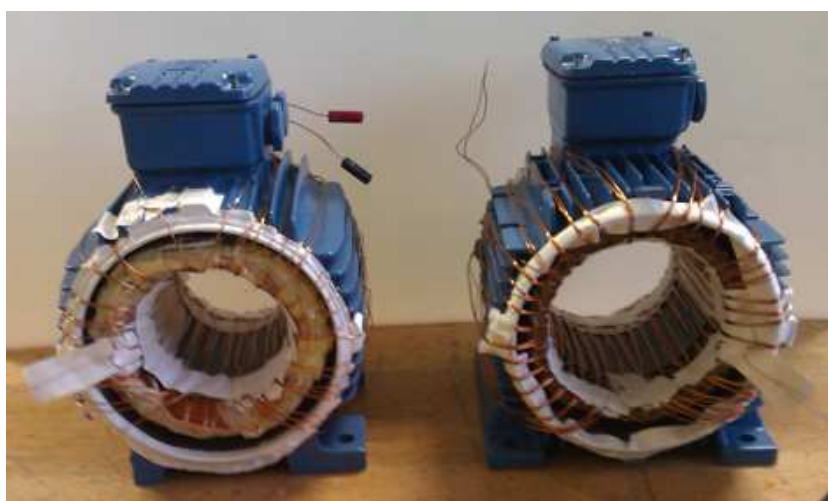


Figure 3: The stators of the 3 kW (left) and 1.5 kW machines, with a distributed excitation winding added around both stator yoke and housing, and a concentrated measurement winding around the stator yoke only. The excitation winding is clearly visible on the picture.

The measurement winding is a concentrated winding that contains the magnetic yoke but not the housing. Then, an excitation winding was added, uniformly distributed along the circumference. The field was obtained from Ampere's law. Hysteresis loops were measured for many amplitudes and frequencies in order to identify the parameters in the static and in the dynamic hysteresis model.

Secondly, from the quasi-static loops (0.5 Hz), the peak H and B values are used to determine the single valued magnetic material characteristic of the stator iron in the FEM. Fig. 4a shows the single valued BH -characteristic used in 2-D FEM.

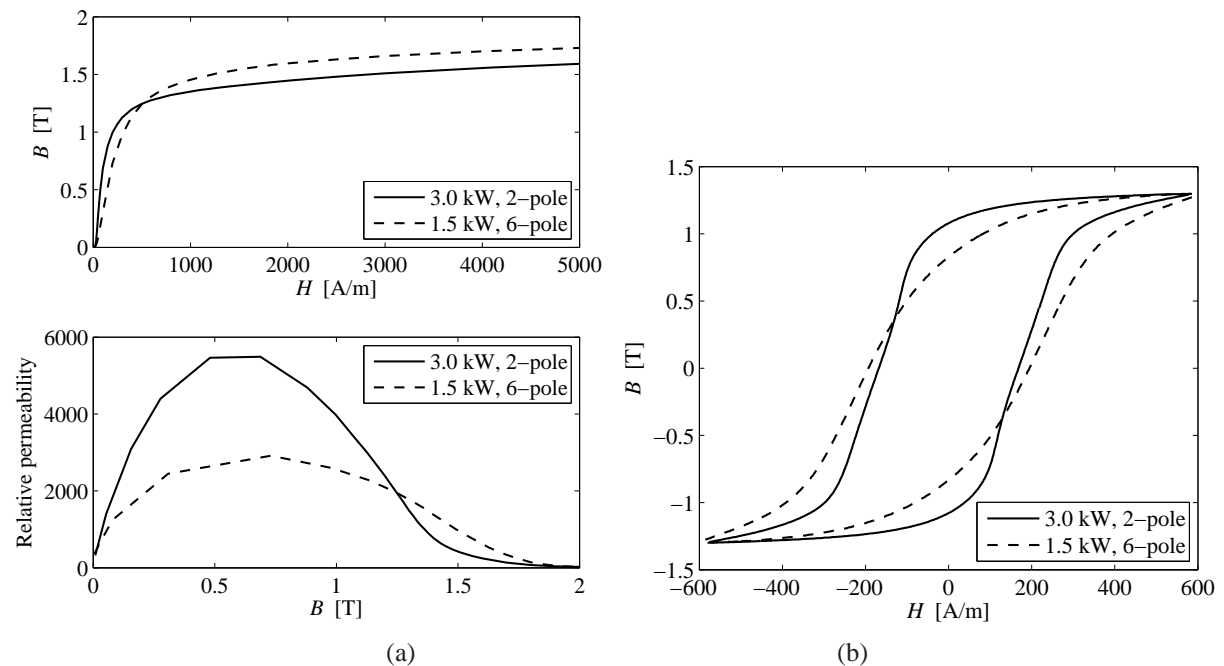


Figure 4: (a) Static single valued characteristic, based on measured hysteresis loops at 0.5 Hz; (b) Measured hysteresis loops at 50 Hz and 1.3 T. The measured loops are obtained by using an excitation and a measurement winding around the stator yoke.

Thirdly, in order to determine the losses, the coefficients a and α in the following equation for hysteresis loss P_h are fitted based on hysteresis loop measurements with peak inductions B_p between 0.05 T and 1.8 T and a frequency of 0.5 Hz:

$$P_h(B_p, f) = aB_p^\alpha f \quad (1)$$

The correspondence between the fitted and the measured losses at 0.5 Hz is very good, with these two parameters. The values of a and α are shown in Table 2.

The dynamic loss model is based on [9]. The iron loss can be written as

$$P(t) = P_h(B_p) + b \left| \frac{dB(t)}{dt} \right|^2 + c\delta \left| \frac{dB(t)}{dt} \right| \left(\sqrt{1 + d \left| \frac{dB(t)}{dt} \right|} - 1 \right) \quad (2)$$

with $P_h(B_p)$ obtained from (1), b , c , and d fitting parameters. If the electrical conductivity σ is known, b can be explicitly computed: $b = \sigma d_{\text{lam}}^2 / 12$ with d_{lam} the lamination sheet thickness.

Table 2: Coefficients in the loss equation for the stator iron

Coefficient	3.0 kW	1.5 kW
	2-pole	6-pole
a	0.0328	0.0351
α	1.9992	1.6709
b	3.266×10^{-5}	3.6758×10^{-5}
c	0	0
d	0	0

The parameters b , c , and d were fitted based on many loops with amplitudes between 0.05 and 1.6 T, and frequencies between 1 Hz and 15000 Hz in order to have an acceptable correspondence in a broad amplitude and frequency range: see Fig. 5a and 5b. Fig. 4b shows a hysteresis loop at 50 Hz, for each motor. As shown in Table 2, coefficients c and d are zero, meaning that the excess loss is negligible.

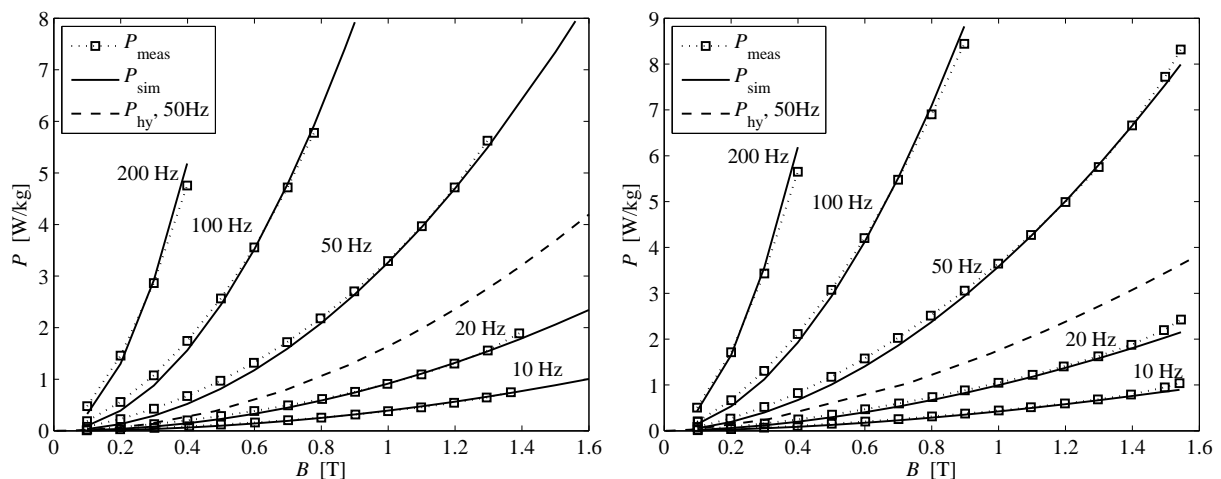


Figure 5: Measured loss on the stator of the machine (rotor removed), and computed loss for the same sinusoidal waveforms. The hysteresis loss component at 50 Hz is shown and can be compared with the total measured loss at 50 Hz.

The loss model to calculate the iron losses in the machine starts from the recorded waveforms $B(t)$ of the 2-D FEM in each considered point of the stator. The loss model integrates the loss function (2) over the domain of the stator iron. In this equation, the hysteresis loss is computed per cycle by (1), based on the peak value B_p of $B(t)$ in each stator point. Minor loops cannot be modelled in this approach, but the transient FEM simulations show that no significant minor loops occur. For the dynamic loss, the loss model computes $\frac{dB(t)}{dt}$ from the waveforms $B(t)$. A non sinusoidal $B(t)$ may result in much higher dynamical losses than a sinusoidal $B(t)$.

The **rotor losses** consist of losses in the magnets and the rotor yoke. The losses originate from space and time harmonics. As the magnets are segmented, the simulations do not take into account the rotor losses.

The **losses in the copper stator windings** can be quite easily computed from the enforced stator current and the (measured) resistance.

4 Efficiency maps

4.1 Experimental setup

The general purpose of this study is to set up an efficiency map of the induction motors and synchronous motors. The test setup consists of the machine under test coupled with a absorption Dynamometer to measure how much torque, power, or speed it can produce. The electrical power of the motor is measured by a Voltech PM6000 power analyzer and the rotation speed of the motor is measured by means of an optical tachometer and by a position encoder with 2500 pulses per revolution. In order to have high accuracy, the efficiency is determined by a direct method – mechanical power on the shaft divided by electrical input power –, and not by indirect methods as specified in IEC standard 60034-2 [10]. Evidently, the IM and PMSM version of the machine were tested using the same stator, and the same setup with the same Foucault brake as load. Only the rotor of the machine was changed.

For the 3 kW IM and PMSM, a perfectly sinusoidal three phase voltage system was used. The voltage waveforms were made by a power source consisting of three linear amplifiers. The frequency and voltage are variable. This eliminates the effect of higher harmonics of e.g. PWM on the losses. For the induction machine, the voltage was rescaled proportionally with the frequency (U/f -control), starting from the nominal frequency and amplitude of the voltage. For the synchronous machine, the voltage was varied in order to obtain the minimal electric power for a given mechanical power. In the measurements, the torque range was 0 – 9 Nm and the speed range was 1200 – 3000 rpm.

For the 1.5 kW machine, a frequency converter was used. The mechanical torques that were applied varied between 0 Nm and 14.5 Nm; the speed range was 0 – 1000 rpm.

4.2 Induction and synchronous machine 3 kW, 2-pole

Fig. 6 shows the measured efficiency map of the induction machine and the PMSM. The supply was a perfect sinusoidal three phase system.

In all measured working points, the PMSM has a higher efficiency than the IM. The average efficiency in the range $0.5 T_{nom} - T_{nom}$ and $0.5 N_{nom} - N_{nom}$ is 83.24% and 85.47% for the induction machine and PMSM respectively, where T_{nom} denotes the nominal torque of 9 Nm and N_{nom} denotes the nominal speed of 3000 rpm.

At low speed and low torque (less than 30% of nominal torque), the efficiency of the converted synchronous machine is much higher than the efficiency of the induction machine: up to 90% efficiency while the induction machine has an efficiency between 70 and 80%. The maximal difference in efficiency is 18% around 1800 rpm and low torque (<2 Nm). For increasing speed and low torque, the difference in efficiency becomes smaller but the PMSM has always at least 6% higher efficiency than the

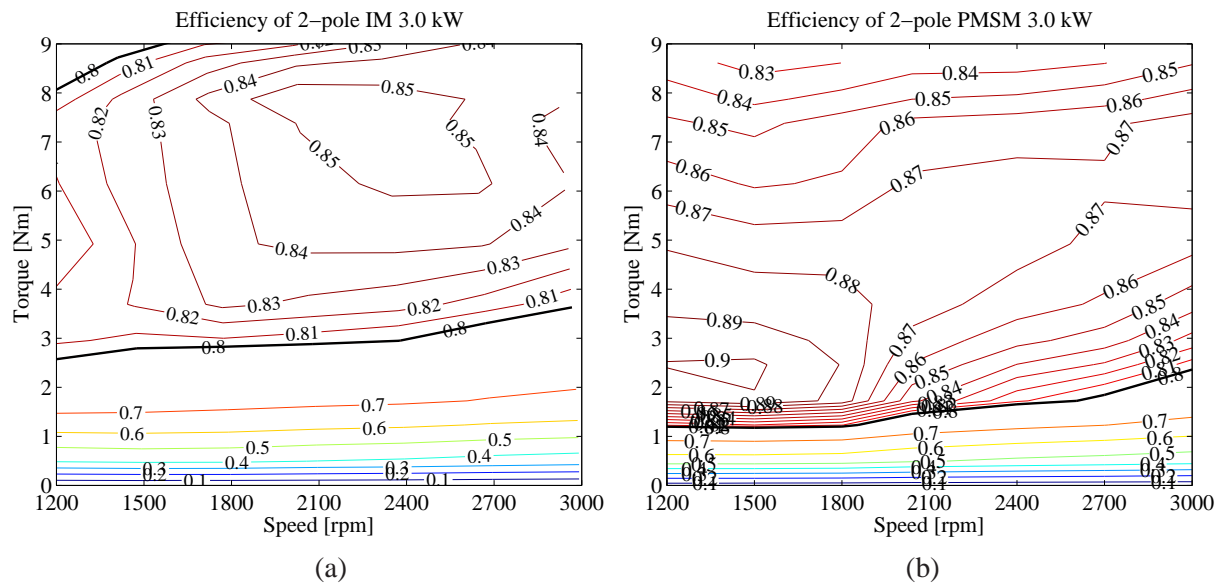


Figure 6: Measured efficiency map of (a) the original commercial 3.0 kW 2-pole induction machine, and (b) the machine converted to PMSM. Note that for clarity of the figure, the contour lines are not equidistant for $\eta < 0.8$.

IM. At high speed and high torque, the difference in efficiency is small (typically 87% for the PMSM, 85% for the IM).

It is noted that the PMSM could even have a higher efficiency: the magnet poles consisting of many rectangular blocks are not optimized for maximal efficiency: they produce space harmonics that are visible in a ripple in the measured and computed EMF waveform – see Fig. 7a – and hence in cogging torque. However, making a segmented magnet with sinusoidal flux distribution in space would increase the cost significantly for a rather small efficiency improvement.

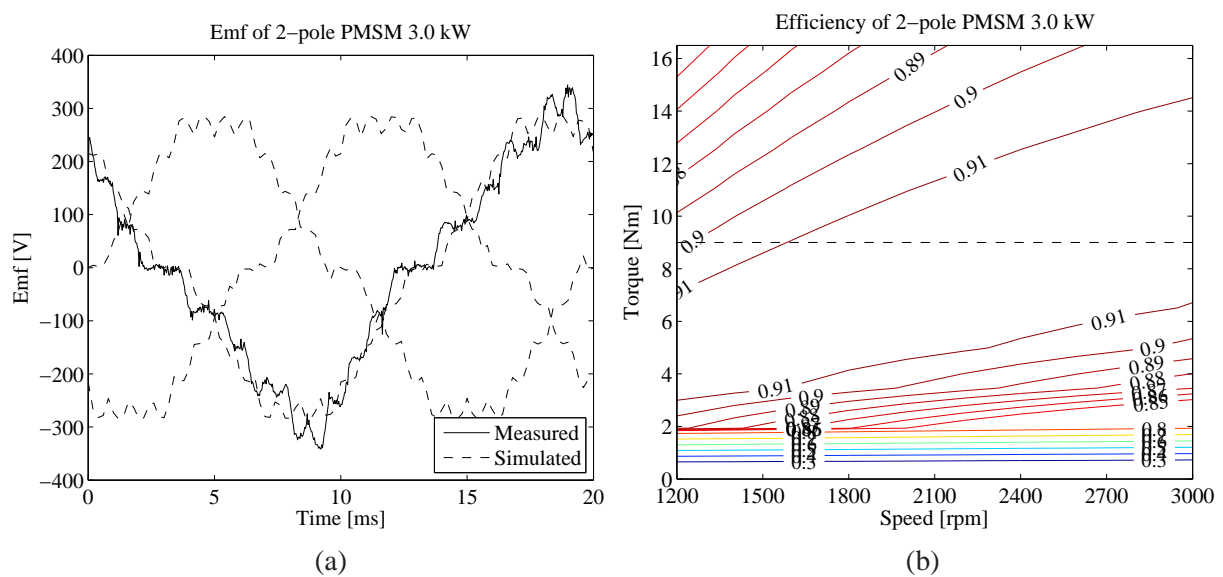


Figure 7: (a) EMF and (b) computed efficiency map of the 3 kW 2-pole synchronous machine. The dashed line shows the nominal torque, which is the maximum in the measured efficiency maps of Fig. 6.

The region of high efficiency can also be tuned by the rotor design. The considered machine has a rather low no-load induction in the iron (1.3-1.4 T), causing low iron losses and a high efficiency for very low torque. This is an “economic” solution from point of view of magnets. Increasing the magnet flux by adding one or two extra rows of magnet blocks per pole increases the iron losses, but reduces the copper losses. This results in a shift of the high efficiency region towards higher torque, especially at higher speed.

Fig. 7b shows the computed efficiency map. The shape of the contour lines corresponds well to the measured map of Fig. 6. The computed efficiency is a bit higher than the measured one, possibly due to neglected rotor losses.

4.3 Induction and synchronous machine 1.5 kW, 6-pole

Fig. 8 shows the measured efficiency map of the induction machine and the PMSM version of the 1.5 kW machine. The supply was a PWM signal with 5 kHz switching frequency.

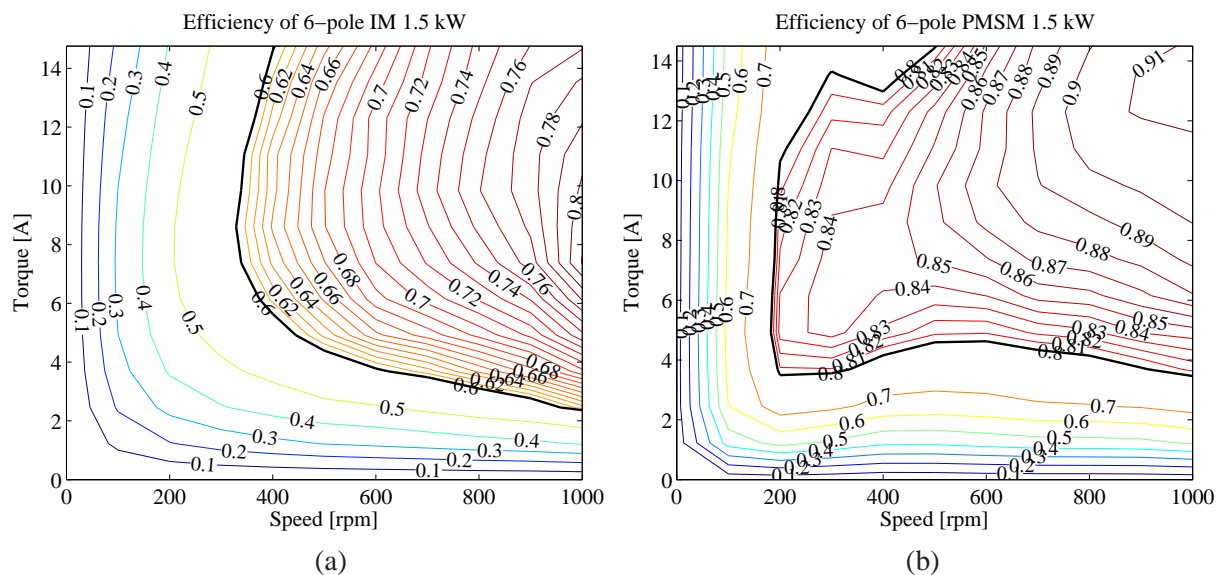


Figure 8: Measured efficiency map of (a) the original commercial 1.5 kW 6-pole induction machine, and (b) the machine converted to PMSM. Note that for clarity of the figure, the contour lines are not equidistant for $\eta < 0.6$ in (a) and $\eta < 0.8$ in (b).

In all measured working points, the PMSM has a higher efficiency than the IM. The average efficiency in the range $0.5 T_{nom} - T_{nom}$ and $0.5 N_{nom} - N_{nom}$ is 73.53% and 88.36% for the induction machine and PMSM respectively, with $T_{nom} = 14.5$ Nm and $N_{nom} = 1000$ rpm. The peak efficiency of the PMSM (91%) is about 11% higher than for the IM. The peak efficiency of the PMSM is reached for the nominal working point, while the induction machine reaches its peak efficiency at nominal speed and about 2/3 of the nominal torque.

Fig. 9a shows the EMF. The simulations were done at steady state temperature (magnet remance 1.05 T),

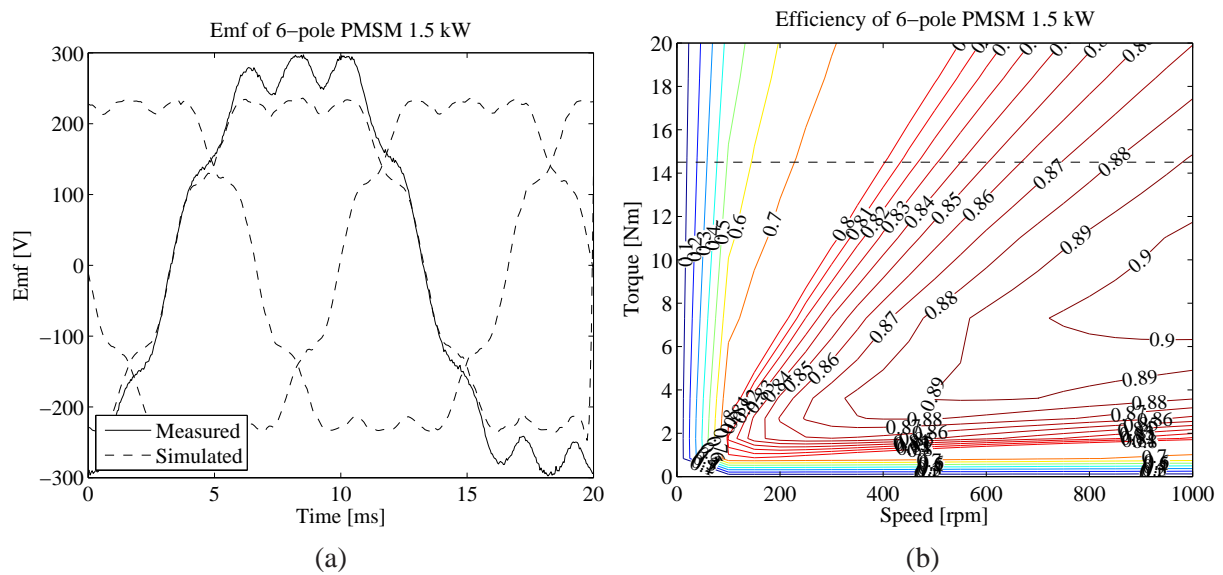


Figure 9: (a) Simulated EMF (at steady state temperature) and measured EMF (cold) and (b) computed efficiency map of the 1.5 kW 6-pole synchronous machine. The dashed line shows the nominal torque, which is the maximum in the measured efficiency maps of Fig. 8.

causing a lower EMF than the measurement which was done at ambient temperature of 20°C (magnet remanence 1.17-1.21 T). The ripple caused by the segmented magnets is visible in both the measured and the simulated waveform. The computed efficiency map for the PMSM in Fig. 9b can be compared with the measured efficiency map of Fig. 8. The correspondence is very good for this machine, which indicates that the remaining part of the rotor cage – which was not modelled in FEM – does not deteriorate the performance.

It is clear that the magnetic circuit is not optimized for the considered machine. Using a low loss material would reduce the iron losses and increase the efficiency in particular at part load. As the rather thin stator yoke saturates even with 1.05 T magnets, a magnet pole angle of only 142° and a rather big air gap of 1.7 mm, it is clear that a new geometry of the induction motor's stator yoke would allow to increase the performance: a thicker stator yoke would allow to use stronger magnets, a higher magnet pole angle and a smaller air gap. It would result in more flux and hence more torque for the same stator current. A design of the lamination for an induction motor has been done in [11], in order to obtain better performance. Future work may include the investigation of changes in geometry and material of the stator.

5 Conclusion

Converting a commercial induction machine to a synchronous machine is a rather cheap and easy conversion. Although it is possible to make an entirely new rotor, experiments show that it is sufficient to reduce the diameter of the rotor without removing the remaining of the rotor cage.

For a 2-pole machine, the average efficiency increases by about 2% in a wide operating range. For the

6-pole machine however, the average efficiency increases by about 15% in a wide operating range. The conclusion is that more efficiency gain is achieved when converting multipole machines. The reason is that small induction machines with many poles are not efficient, so that a lot of improvement is possible.

6 Acknowledgment

This work was supported by the Research Fund of University College Ghent, by the GOA project BOF 07/GOA/006 and the IAP project P6/21. The second author is a postdoctoral researcher for the “Fund of Scientific Research Flanders” (FWO).

References

- [1] Rotating electrical machines – Part 30: Efficiency classes of single-speed, three-phase, cage induction motors (IE-code). IEC Standard 600034-30, (2008-10), 2008
- [2] Stockman, K., Dereyne, S., Vanhooydonck, D., Symens, W., Lemmens, J., Deprez, W.: “Iso efficiency contour measurement results for variable speed drives”, *International conference on electrical machines (ICEM 2010)*, Rome, Italy, September 6-8, 2010, paper RF-009873, cd-rom
- [3] Kikuchi, S.; Takahashi, A.; Mikami, H.; Wakui, S.; Kou, H.; Tanaka, K.; Miyake, M.; Yoshikawa, T.; Tojo, K.: “Development of self-starting permanent magnet synchronous motors for compressor drives,” *Proc. 12th International Conference on Electrical Machines and Systems (ICEMS 2009)*, Tokyo, Japan, 15-18 November 2009
- [4] Krol, E.: “Comparison of energy efficiency of permanent magnet synchronous motors and induction motors,” *Maszyny Elektryczne*, 2007, **78**, pp. 75-78
- [5] Gessese, Y., Binder, A.: “Axially slitted, high-speed solid-rotor induction motor technology with copper end-rings,” *12th International Conference on Electrical Machines and Systems (ICEMS 2009)*, Tokyo, Japan, 15-18 November 2009
- [6] Wang, K., Jin, M.J., Shen, J.X., and Hao, H.: “Study on rotor structure with different magnet assembly in high-speed sensorless brushless DC motors,” *IET Electric Power Applications*, 2010, **4**, (4), pp. 241-248
- [7] Wang, Y., Cheng, M., Chen, M., Du, Y., and Chau, K. T.: “Design of high-torque-density double-stator permanent magnet brushless motors,” *IET Electric Power Applications*, 2011, **5**, (3), pp. 317-323

- [8] Crevecoeur, G., Sergeant, P., Dupré, L., Vandenbossche, L., and Van de Walle, R.: “Analysis of the local material degradation near cutting edges of electrical steel sheets”, *IEEE Transactions on Magnetics*, 2008, **44**, (11), pp. 3173-3176
- [9] Barbisio E., Fiorillo F., and Ragusa C.: “Predicting Loss in Magnetic Steels Under Arbitrary Induction Waveform and With Minor Hysteresis Loops,” *IEEE Transactions on Magnetics*, 2004, **40**, pp. 1810-1819
- [10] Rotating electrical machines – Part 2: Methods for determining losses and efficiency from tests (excluding machines for traction vehicles). IEC Standard 60034-2, 2007
- [11] Alberti, L., Bianchi, N., Bolognani, S.: “Lamination design of a set of induction motors”, *Journal of Electrical Engineering: Theory and application*, 2010, **1**, pp. 18-23